Jet momentum dependence of jet quenching in PbPb collisions at $\sqrt{s_{NN}}$ = 2.76 TeV

CMS Collaboration

Physics Letters B 712 (2012) 176–197

Presented as student project on behalf of Group A

by Simon Heisterkamp

at AEPSHEP on 25 Oct. 2012

Motivaton

- Study of Heavy Ion collisions
- QGP is a ‘coloured’ liquid
- partons themselves act as probes

→ observable as jet quenching

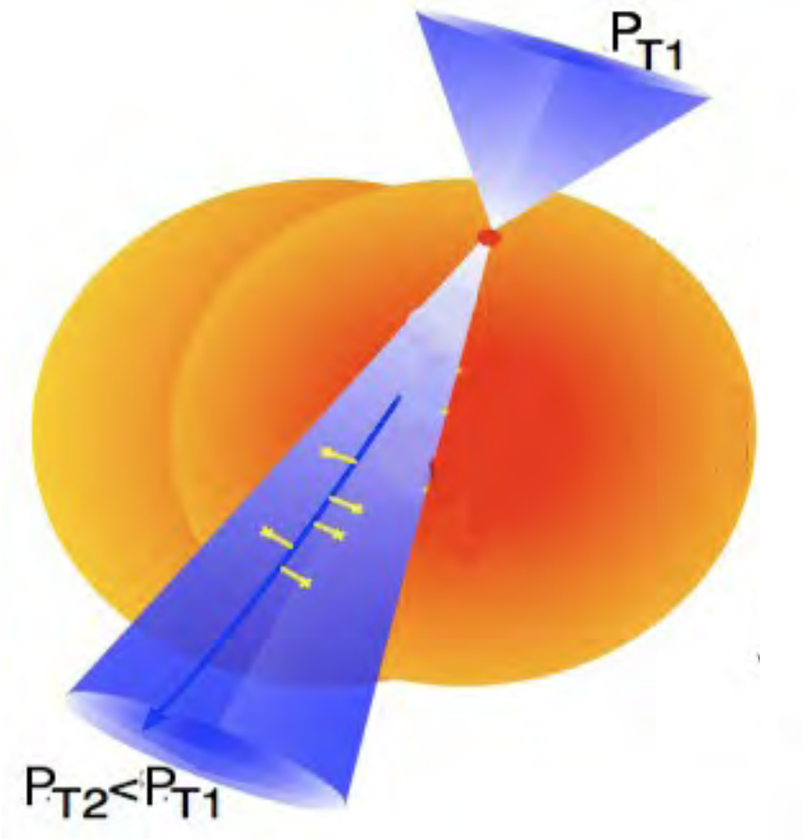

Motivaton

Motivaton

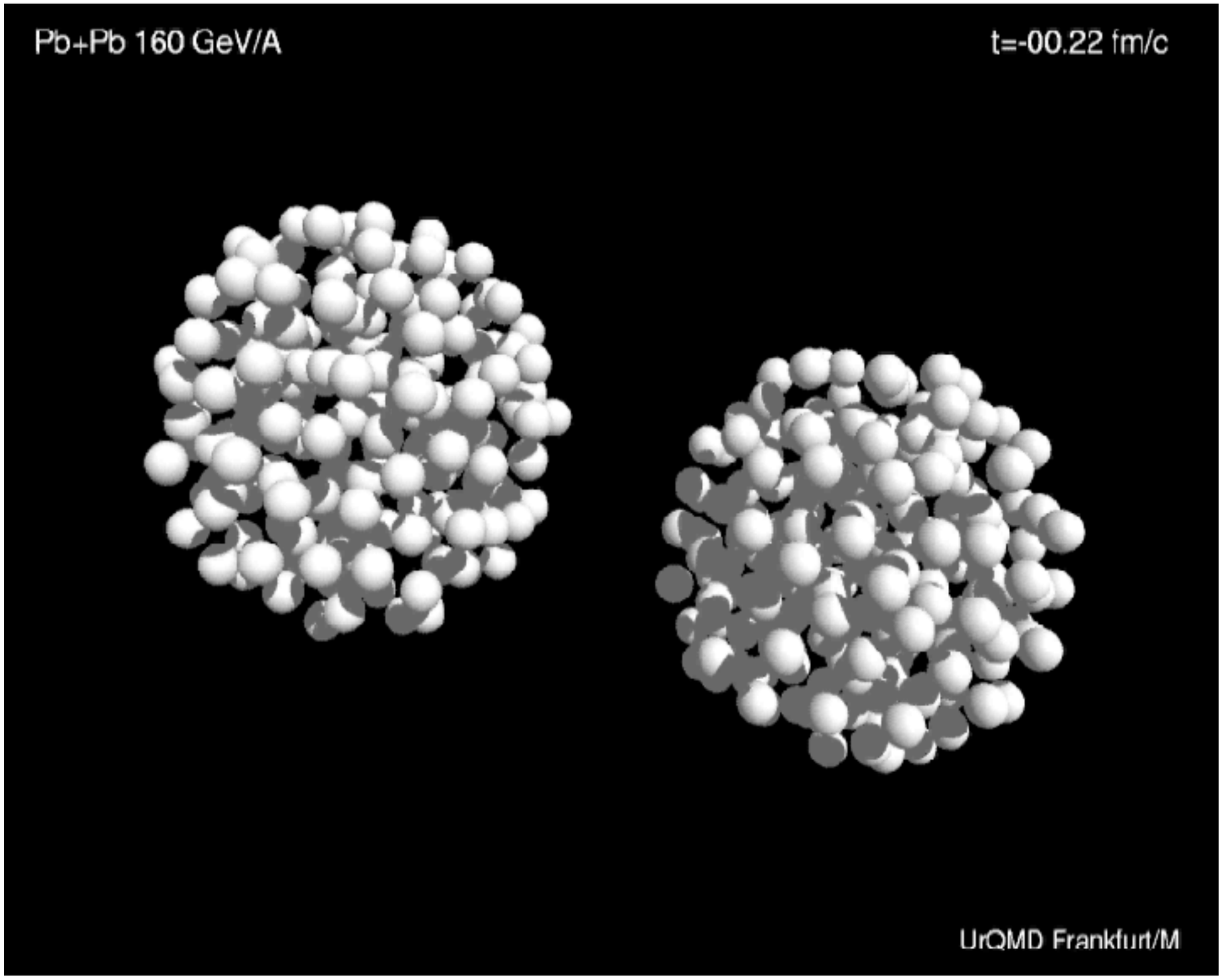

Motivaton

- Study of Heavy Ion collisions
- QGP is a 'coloured' liquid
- partons themselves act as probes

  → observable as jet quenching

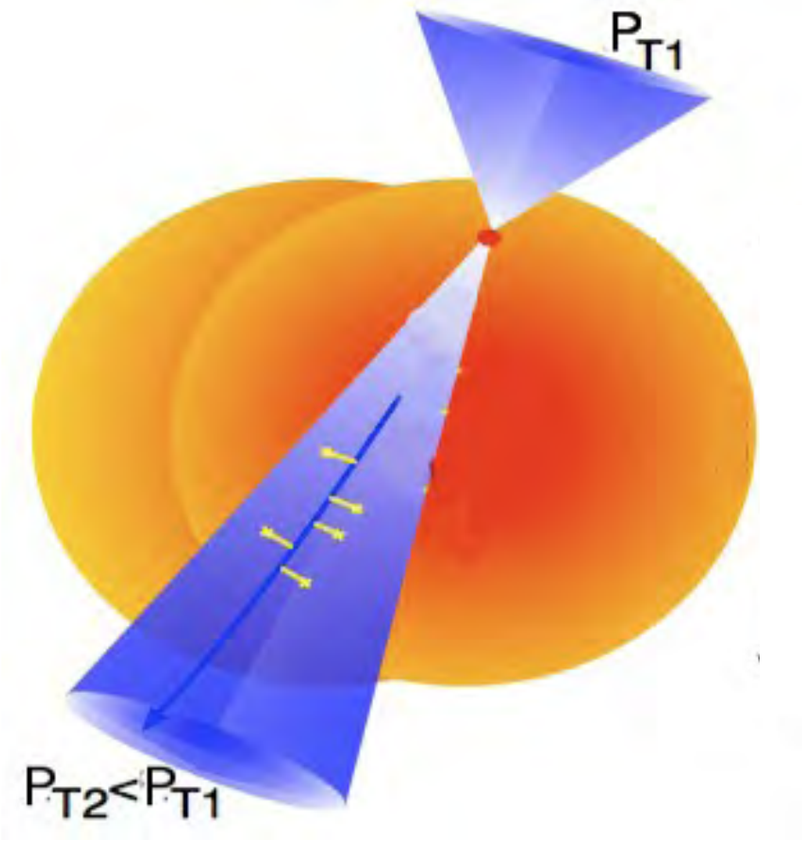

- Observables: $p_{T,2}/p_{T,1}$ $A_J=(p_{T,1}-p_{T,2})/(p_{T,1}+p_{T,2})$
- lower ratio* = higher A_J* = quenched recoiling jet

  *(than in pp)

- Simulation:
  - Underlying event: HYDJET
  - Hard process: PYTHIA

→ superimpose

CMS Detector

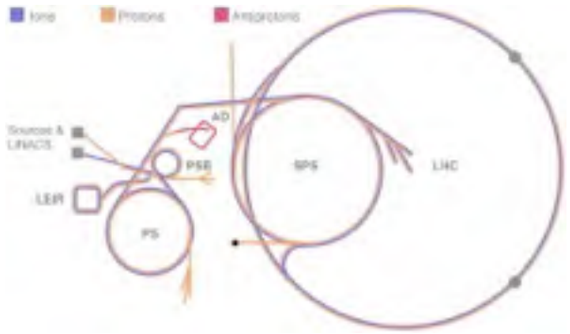

- at the LHC at CERN
- general purpose detector
- can be used for AA
- used 150 $\mu b^{-1} \rightarrow$ 370k evts.

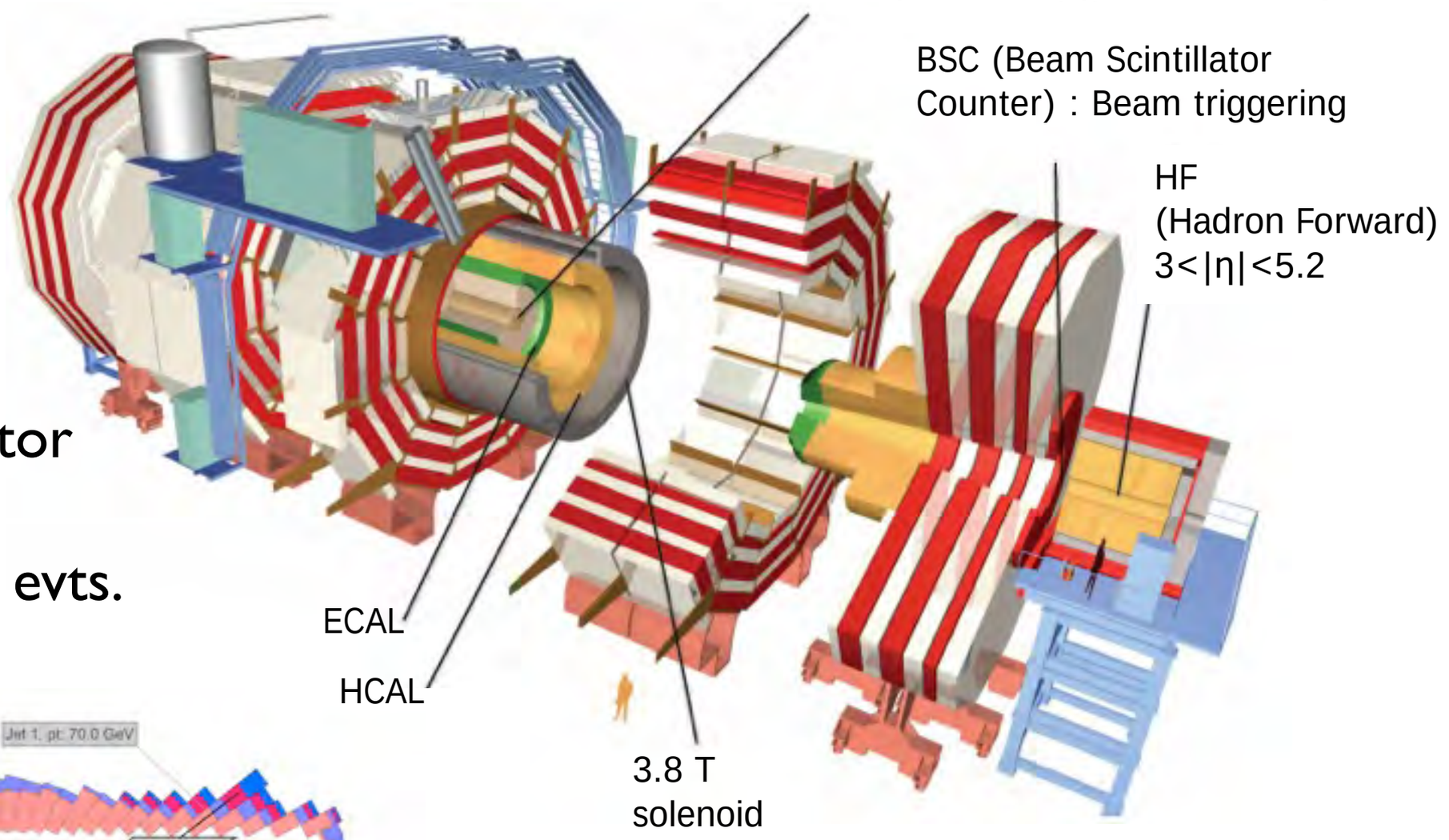

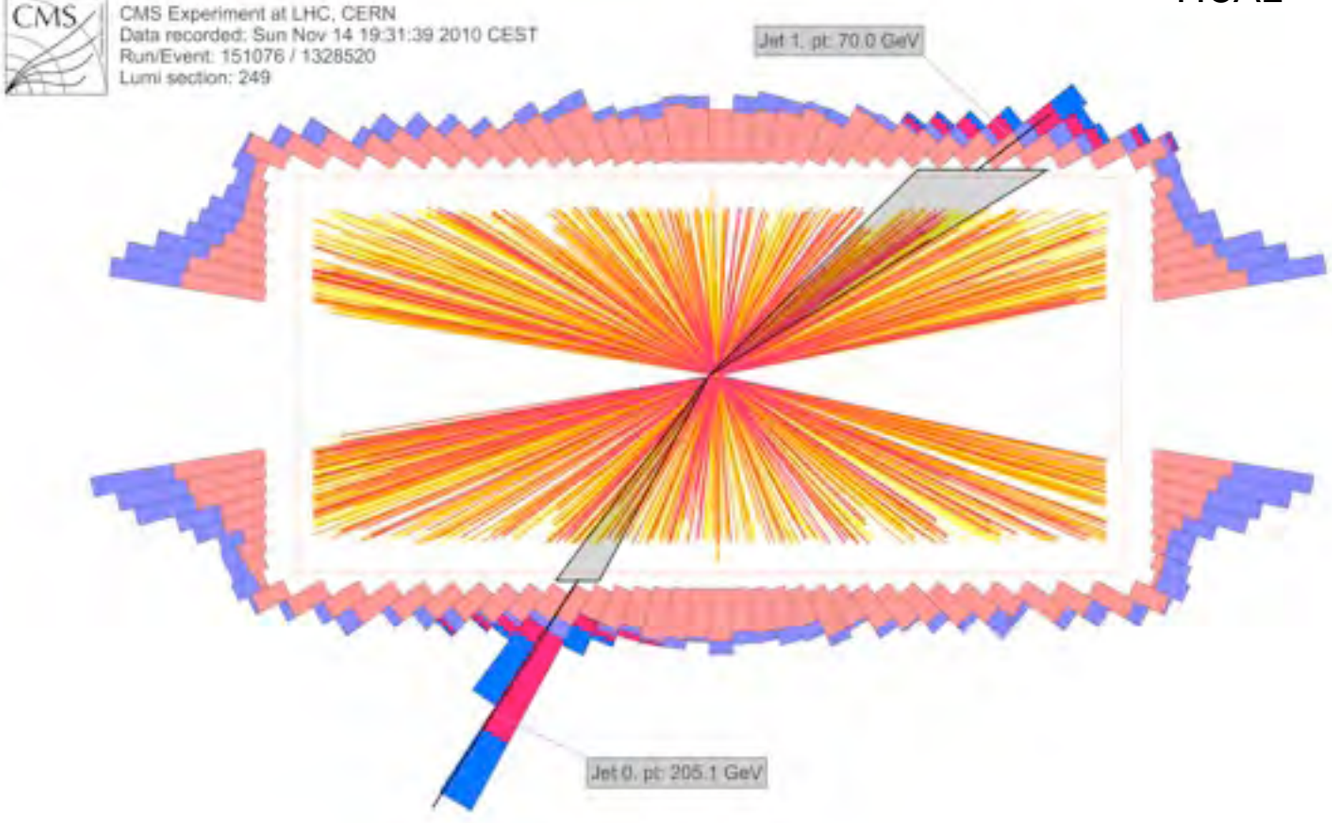

- Jet reconstruction: anti-k_T R=0.3
- Centrality: HF calorimeter

Event Selection

Selection	% of triggered
trigger jet p_T>80GeV	100.0
collision detection	84.0
calorimeter noise rejection	83.4
$p_{T,1}$ > 120 GeV	15.1
$p_{T,2}$ > 30 GeV	14.2
$\Delta\varphi_{1,2} > 2\pi/3$	13.5
track within jet	13.26

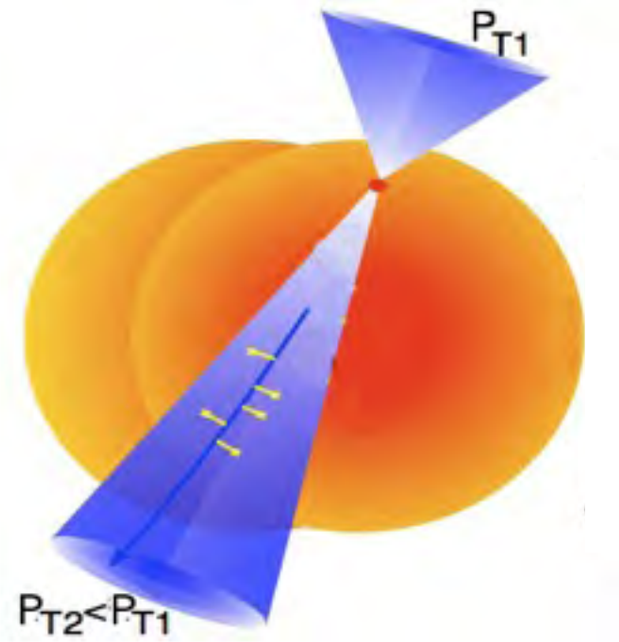

- Centrality:

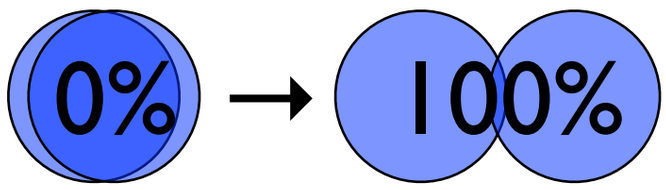

Analysis

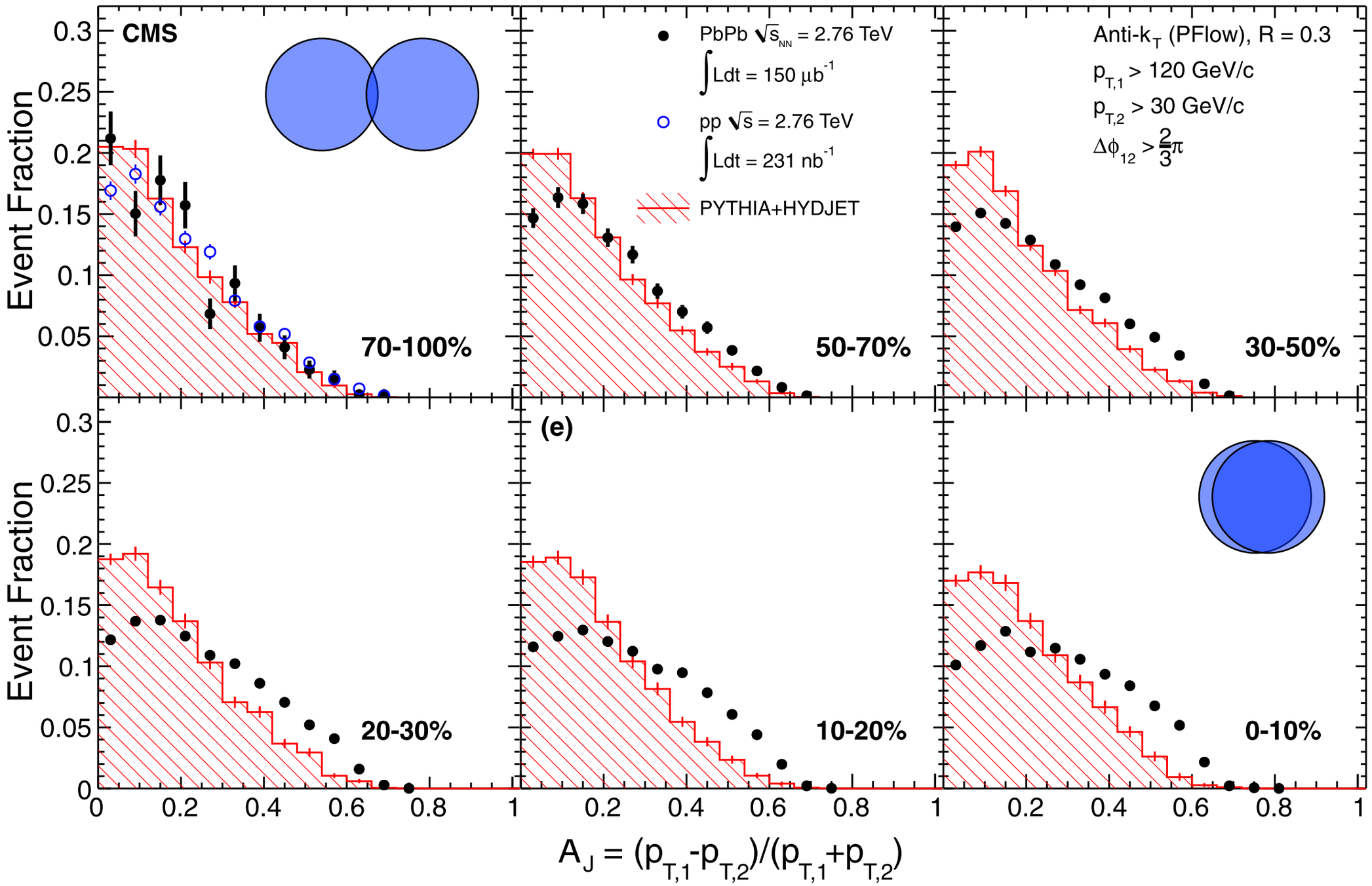
CMS
PbPb √s_NN = 2.76 TeV
∫Ldt = 150 μb^-1
pp √s = 2.76 TeV
∫Ldt = 231 nb^-1
PYTHIA+HYDJET
Anti-k_T (PFlow), R = 0.3
p_T,1 > 120 GeV/c
p_T,2 > 30 GeV/c
Δφ_12 > 2/3π
70-100%
50-70%
30-50%
20-30%
10-20%
0-10%
(e)
Event Fraction
A_J = (p_T,1-p_T,2)/(p_T,1+p_T,2)

Analysis

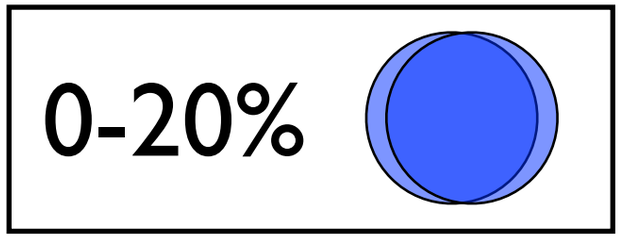
0-20%

CMS
∫Ldt = 150 μb⁻¹
PbPb √s_NN = 2.76 TeV
PYTHIA+HYDJET
Anti-k_T (PFlow), R = 0.3
p_T,2 > 30 GeV/c
Δφ_12 > 2/3π
Centrality 0-20%
120 < p_T,1 < 150 GeV/c
150 < p_T,1 < 180 GeV/c
180 < p_T,1 < 220 GeV/c
220 < p_T,1 < 260 GeV/c
260 < p_T,1 < 300 GeV/c
300 < p_T,1 < 500 GeV/c
⟨p_T,1/p_T,2⟩ PbPb
⟨p_T,1/p_T,2⟩ PYTHIA+HYDJET
Event Fraction
p_T,2/p_T,1

Results

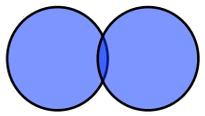

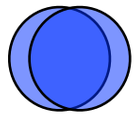

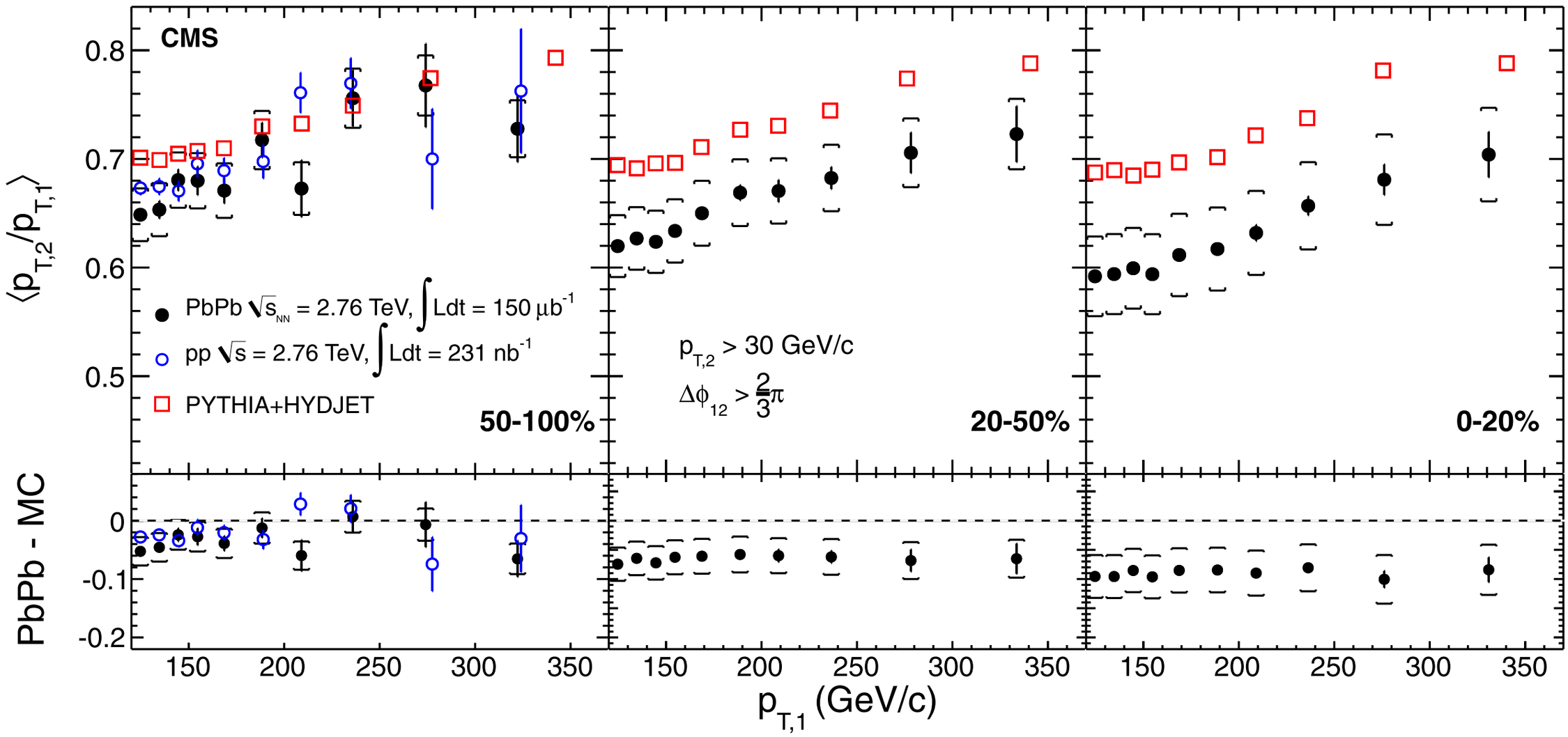

Systematics:

- Underlying event
- Jet energy scale
- Jet efficiency

Conclusions:

- Update confirms earlier work
- more bins of centrality & p_T


THE
A
TEAM

Backup Slides

Analysis

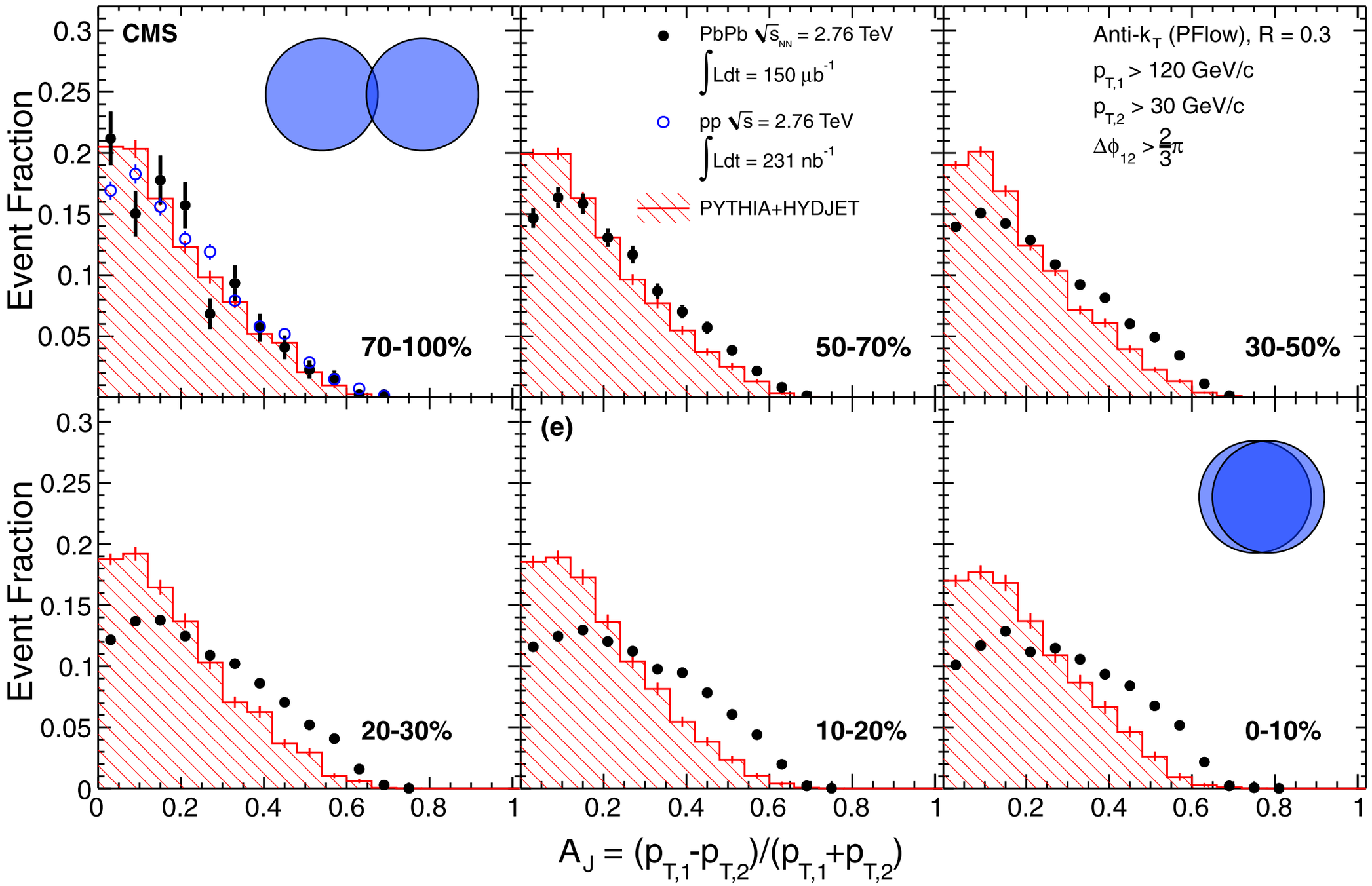
CMS
PbPb √s_NN = 2.76 TeV
∫Ldt = 150 μb^-1
pp √s = 2.76 TeV
∫Ldt = 231 nb^-1
PYTHIA+HYDJET
Anti-k_T (PFlow), R = 0.3
p_T,1 > 120 GeV/c
p_T,2 > 30 GeV/c
Δφ_12 > 2/3π
70-100%
50-70%
30-50%
20-30%
10-20%
0-10%
(e)
Event Fraction
A_J = (p_T,1-p_T,2)/(p_T,1+p_T,2)

Anti k_T

$$d_{ij} = \min(p_{T,i}^{-2}, p_{T,j}^{-2}) \frac{\Delta R_{ij}^2}{D^2}$$

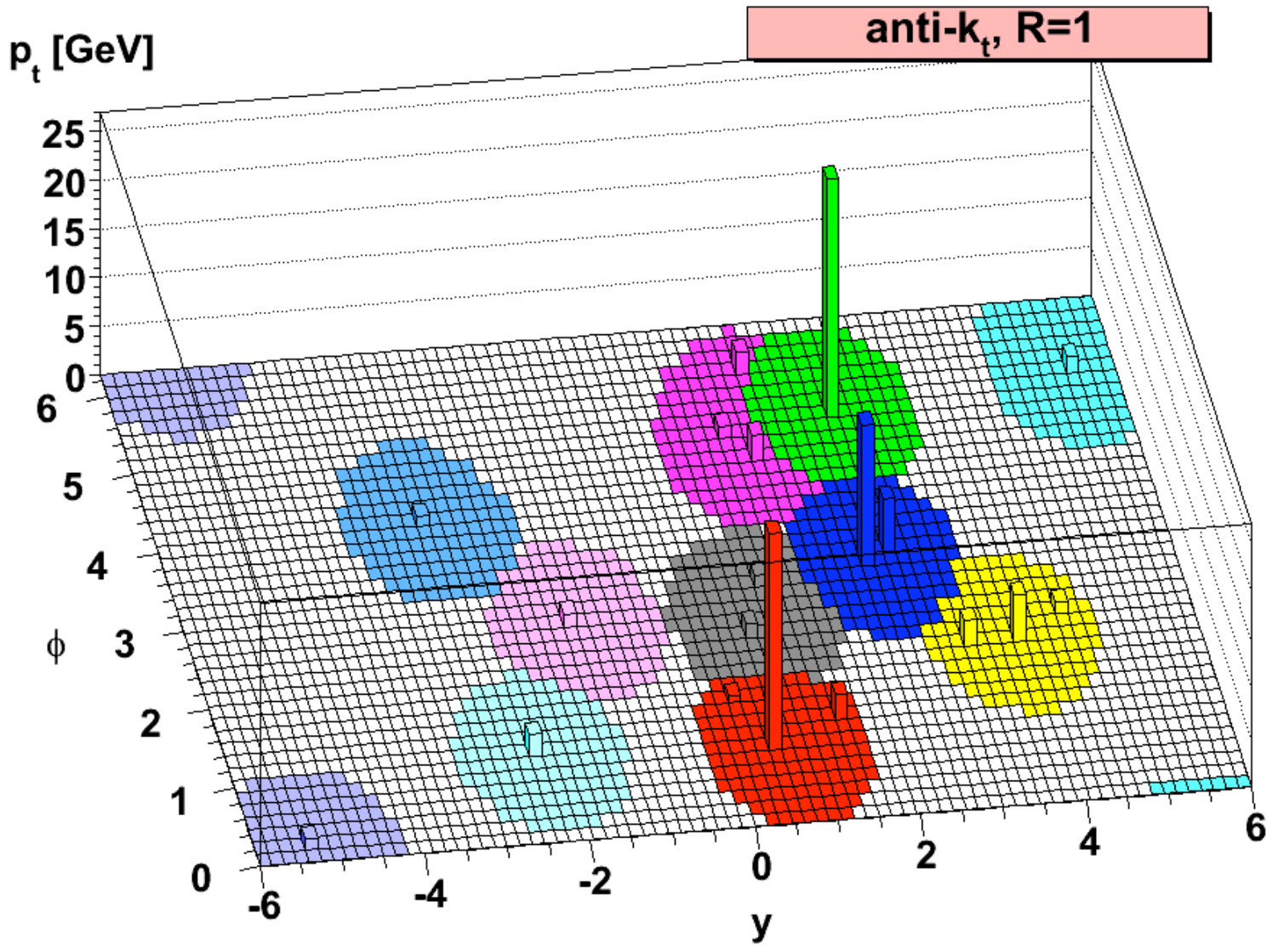

Introduction / Theoretical Motivation

•Quark Gluon Plasma (QGP) is a state of matter consisting of deconfined quarks and gluons that is predicted by Lattice QCD and is recreated (Tc ~ 150-175 MeV & εc ~ 1Gev/fm3) at Relativistic Heavy Ion Collisions at RHIC and LHC.

•Jet quenching is an important observable of QGP at heavy-ion collision that is produced when a hard scattered parton experiences energy loss due to strong interaction with surrounding QGP medium.

•Experimental observable used to identify jet quenching:

- Dijet Asymmetry:

$$A_J = \frac{p_{T,1} - p_{T,2}}{p_{T,1} + p_{T,2}}$$

- Subleading jet transverse momentum fraction:

$$\frac{p_{T,2}}{p_{T,2}}$$

•Differences between the observables obtained in Pb-Pb and that in p-p collisions attributed to the effects due to the medium created during the collisions of the heavy ions.

•PYTHIA+HYDJET MC generates dijet events with particle multiplicities and underlying event effect expected in Pb-Pb data. Differences between Data and MC can be attributed to medium induced effects such as jet quenching.

•Study of dijet properties associated with jet quenching can provide information about properties of QGP

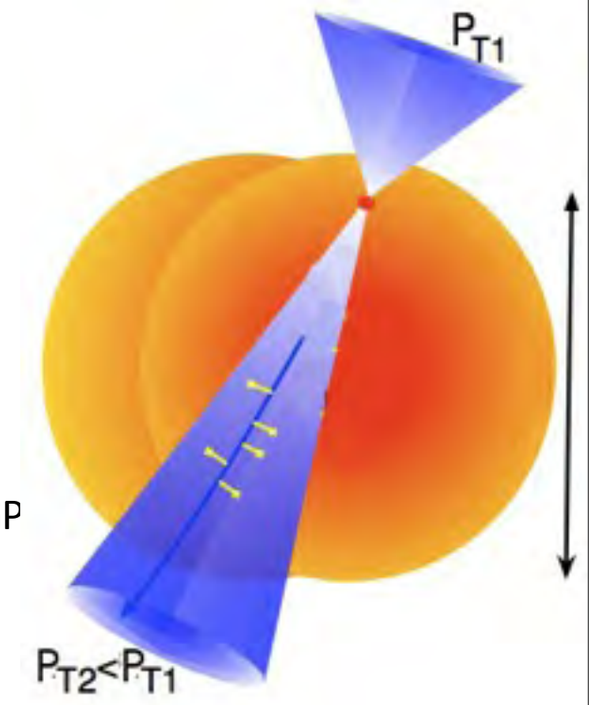

Introduction / Theoretical Motivation

•Quark Gluon Plasma (QGP) is a state of matter consisting of deconfined quarks and gluons that is predicted by Lattice QCD.
•QGP state occurs at Tc (Critical Temperature) ~ 150-175 MeV corresponding to energy density ~ 1Gev/fm3, which was present in the early universe (~10^-6s after Big Bang) and is recreated at Relativistic Heavy Ion Collisions at RHIC and LHC.
•Jet quenching is an important observable of QGP at heavy-ion collision.
•Jet is 'quenched' as the hard scattered parton experiences energy loss due to strong interaction with surrounding QGP medium. Energy loss occurs by way of medium induced gluon emission.
•In di-jet events, where one of the jets emanates from near the surface of region of interaction and the other jet passes through the bulk of the interaction region and gets quenched, the quenched jet has a comparatively lower transverse momentum giving rise to momentum imbalance between the leading and the sub-leading jet.
•Experimental observable used to identify jet quenching:
- Dijet Asymmetry:

$$A_J = \frac{p_{T,1} - p_{T,2}}{p_{T,1} + p_{T,2}}$$

- Subleading jet transverse momentum fraction: $\frac{p_{T,2}}{p_{T,2}}$

•Comparison of the observable in Pb-Pb (Nucleus-Nucleus) collisions and that in p-p collisions are made so that the differences can be attributed to the effects due to the medium created during the collisions of the heavy ions.
•Data is compared to MC simulation using PYTHIA+HYDJET. PYTHIA is used to generate dijet events and HYDJET is tuned to produce particle multiplicities and underlying event effect expected in Pb-Pb data. (Any difference between Data and MC can be attributed to medium induced effects such as Jet Quenching)
•Recent p-Pb collisions at LHC indicate that Jet quenching is not an effect of initial state effect
•Different models for interaction of partons and QGP compare Jet quenching behavior as a function of pT of leading jet to LHC and RHIC data.
•The study of medium-induced effects in dijet properties such as as jet quenching can provide information about the properties of QGP such as transport properties of QGP medium.

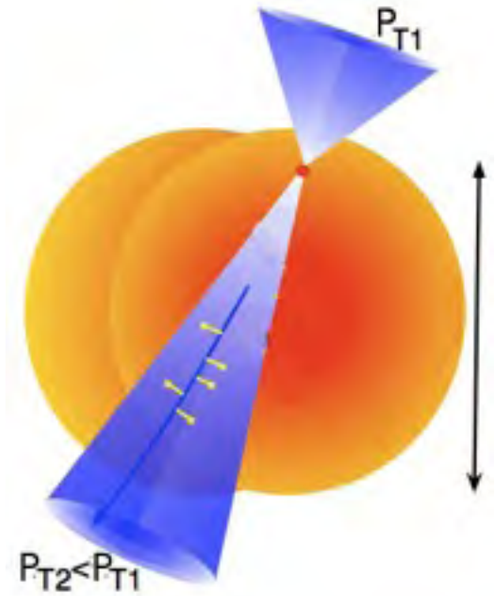

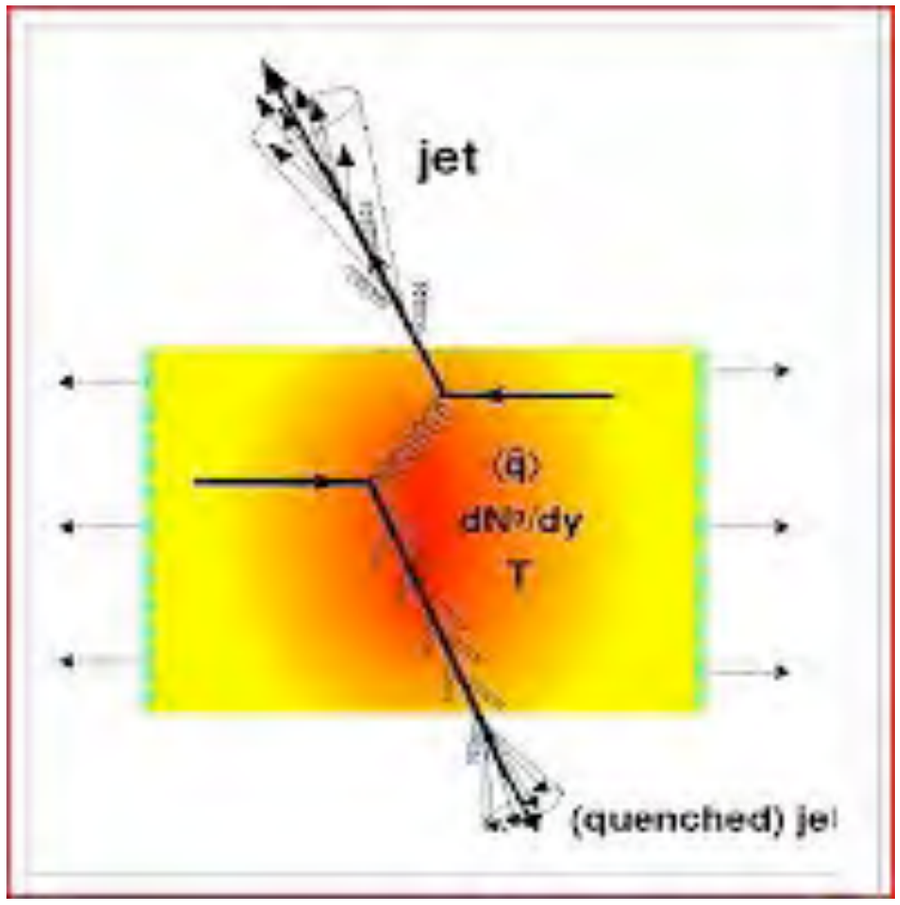

$$A_J = \frac{p_{T,1} - p_{T,2}}{p_{T,1} + p_{T,2}}$$

$$\frac{p_{T,2}}{p_{T,2}}$$

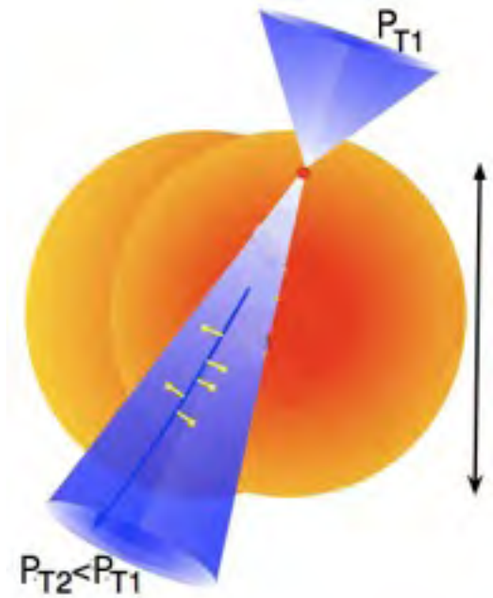

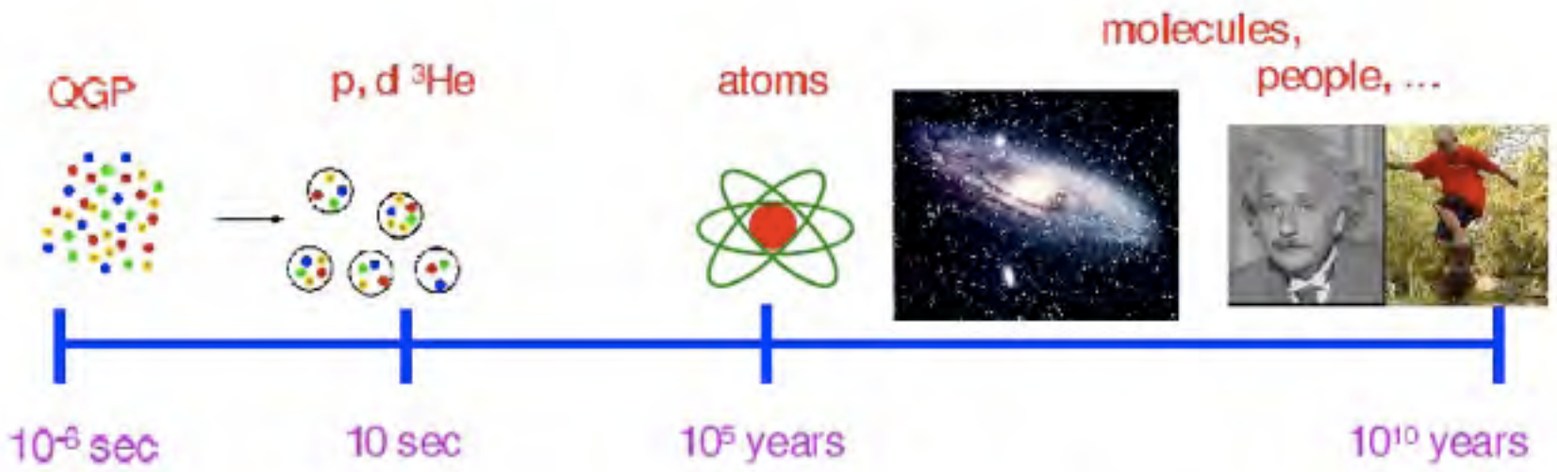

Figure 2.1: History of the universe for temperatures less than $k_B T \sim 100$ GeV.

CMS DETECTOR

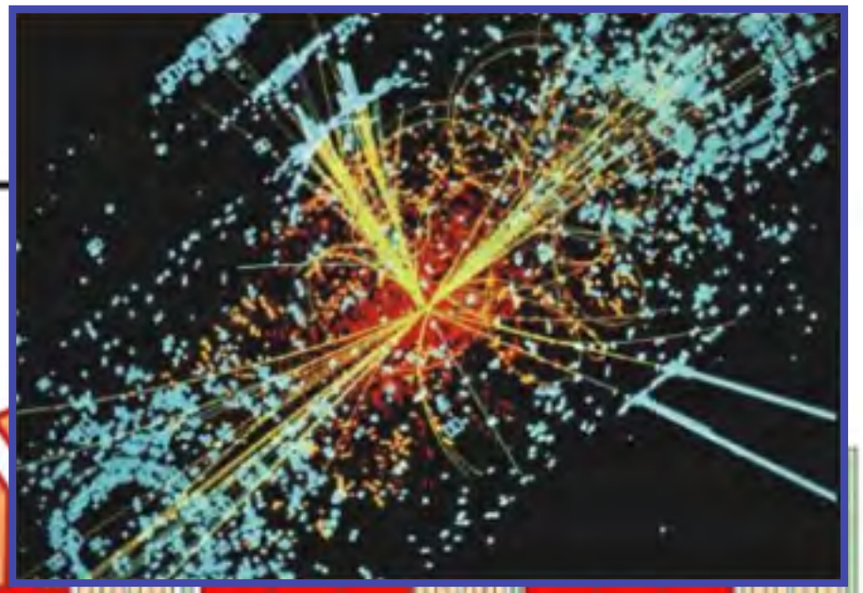

Centrality: HF (Hadron Forward, $3<|\eta|<5.2$)

Jet reconstruction

Jet measurement

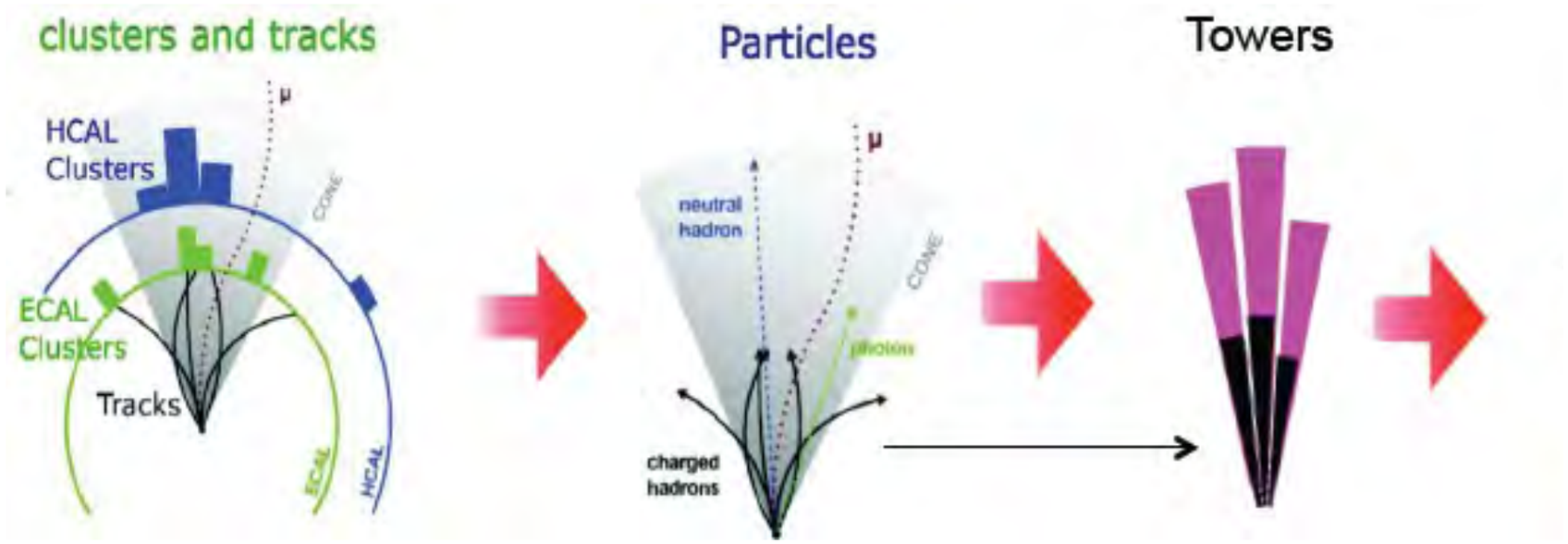

Jet Algorithm:
anti-k_T R=0.3

Underlying Event subtraction

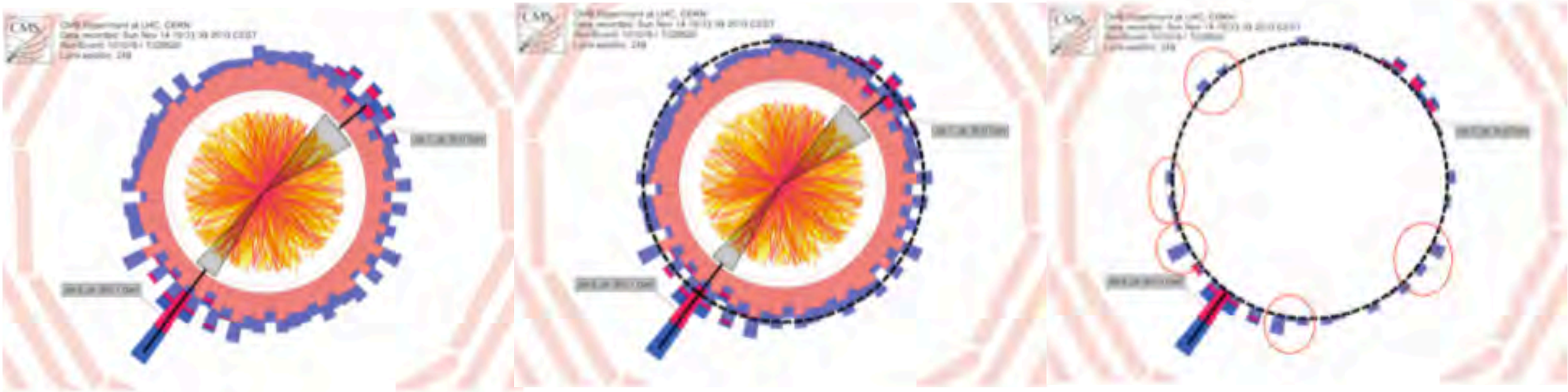

2

Centrality

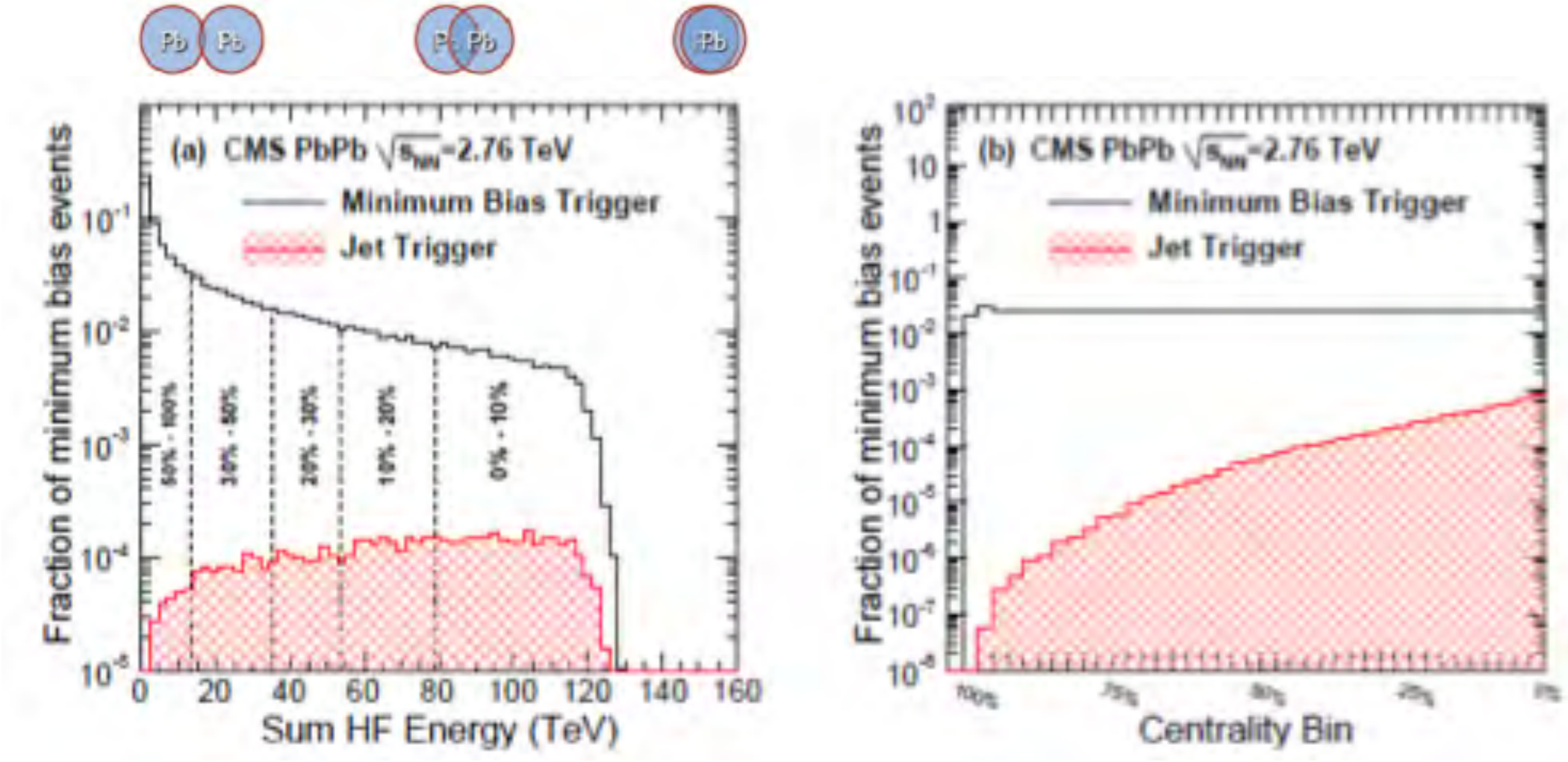

Most peripheral ← 70-100%, 50-70%, 30-50%, 20-30%, 10-20%, 0-10% → Most central

N_{part}: number of participating of nucleons in event

Transverse energy in the HF is correlated to N_{part}

CMS DETECTOR

Silicon Pixel + Strip Tracker |η|<2.5:
Tracking

BSC (Beam Scintillator Counter) :
Beam triggering

HF (Hadron Forward)
3<|η|<5.2 :
Centrality

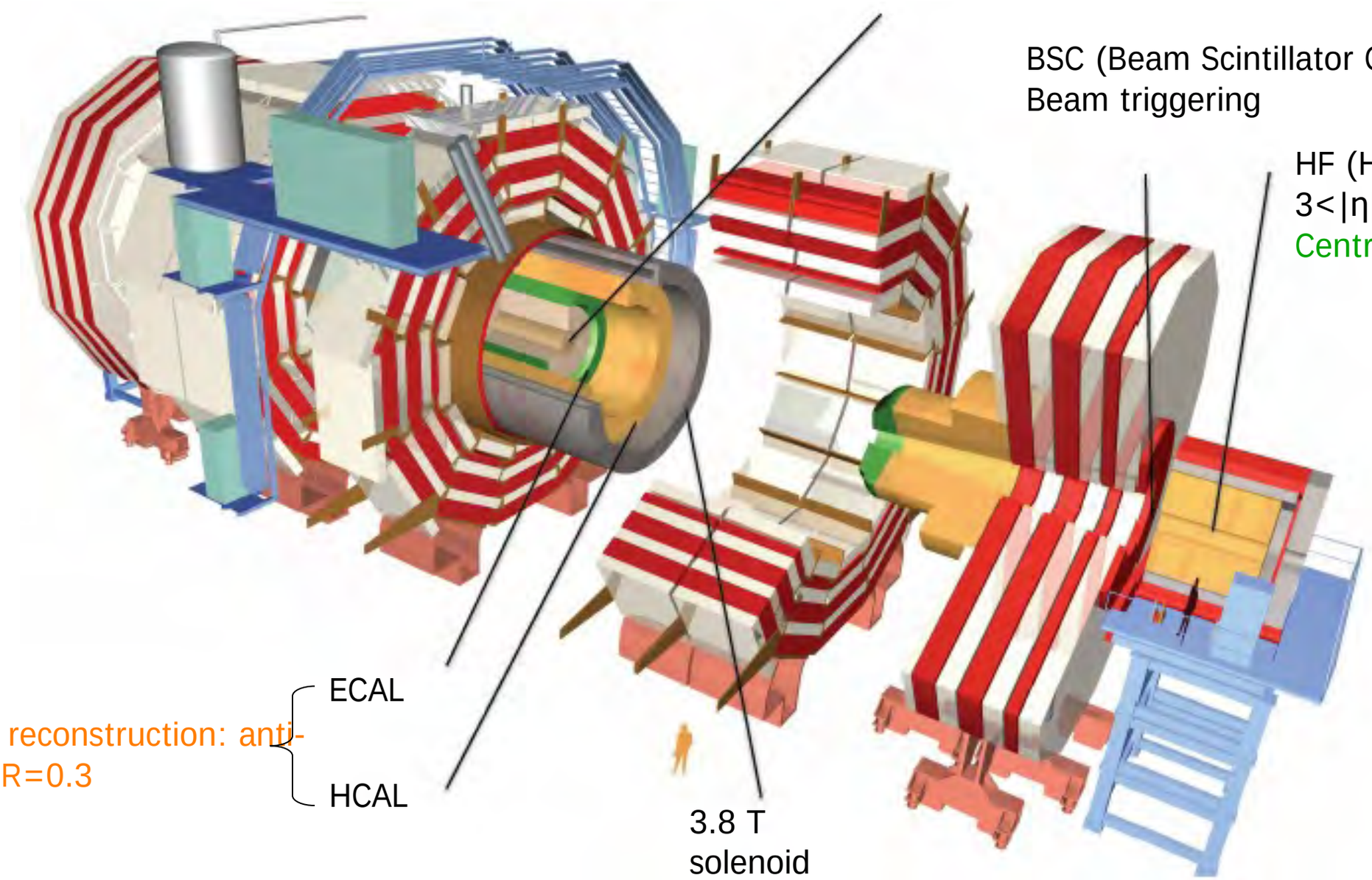

Jet reconstruction: anti-kT R=0.3

ECAL

HCAL

3.8 T
solenoid

Event Selection

- For the suppression of background effects
  - Events with appropriate timing, signal on BSC
  - VX reconstructed by more than 2 tracks with pT > 75MeV is compatible with the length of the pixel clusters
- For the selection of leading & sub-leading jets
  - $|\eta| < 2$
  - At least one track has pT > 120GeV/c
  - pT > 30GeV/c for the sub-leading jet
  - More than $2\pi/3$ for the angle between the leading and sub-leading jets
  - Both jets have at least one track with pT > 4GeV/c

Table 1: The effects of various selections applied to the data sample → fractional values with respect to the triggered sample; the selections are applied in sequence

1) *jet trigger events*: p_T^corrected > 80 GeV/c
inclusive single-jet trigger, corrected for p_T dependent calorimeter energy response, large p_T ensures that particle was produced close to the surface

2) *offline collision selection*
Remove beam-related backgrounds (beam-halo events, beam gas, ultraperipheral collisions), in general events that don't originate from IP

3) *HCAL and ECAL noise rejection*
Remove contamination of noise from had. and e.m. calorimeter using signal timing, energy distribution, pulse shape

4) *leading jet* p_T1 > 120 GeV/c, pseudorapidity |eta| < 2

5) *subleading jet* p_T2 > 30 GeV/c, pseudorapidity |eta| <2

6) Delta Phi > 2pi/3
Azimuthal angle between leading and subleading jet, further jets not considered in this analysis

7) track within jet
Remove residual hadronic calorimeter noise missed by rejection algorithm by requiring a > 4GeV track in either leading or subleading jet

Selections	% of triggered
Jet trigger events p_T^corr > 80 GeV	100.0
Offline collision selection	84.01
HCAL, ECAL noise rejection	83.38
Leading jet p_T1 > 120 GeV	15.11
Subleading jet p_T2 > 30 GeV	14.24
Delta Phi_1,2 > 2pi/3	13.51
Track within jet	13.26

Table 1
The effects of various selections applied to the data sample. In the third column, the fractional values are with respect to the line above and in the fourth column they are with respect to the triggered sample. The selections are applied in sequence.

Selections	Events remaining	% of previous	% of triggered
Jet triggered events ($p_{\mathrm{T}}^{\mathrm{corr}} > 80$ GeV/c)	369 938	100.00	100.00
Offline collision selection	310 792	84.01	84.01
HCAL and ECAL noise rejection	308 453	99.25	83.38
Leading jet $p_{\mathrm{T},1} > 120$ GeV/c	55 911	18.13	15.11
Subleading jet $p_{\mathrm{T},2} > 30$ GeV/c	52 694	94.25	14.24
$\Delta\phi_{1,2} > 2\pi/3$	49 993	94.87	13.51
Track within a jet	49 054	98.12	13.26

Table 2
Summary of the $p_{T,2}/p_{T,1}$ systematic uncertainties. The range of values represent the variation from low ($p_{T,1} < 140$ GeV/c) to high ($p_{T,1} > 300$ GeV/c) leading jet p_T.

Source	50–100%	20–50%	0–20%
Underlying event	1%	3%	5%
Jet energy scale	3%	3%	3%
Jet efficiency	1–0.1%	1–0.1%	1–0.1%
Jet misidentification	$< 0.1\%$	$< 0.1\%$	1–0.1%
Calorimeter noise	$< 0.1\%$	$< 0.1\%$	$< 0.1\%$
Jet identification	$< 0.1\%$	$< 0.1\%$	$< 0.1\%$
Total	3.5%	4.5%	6%

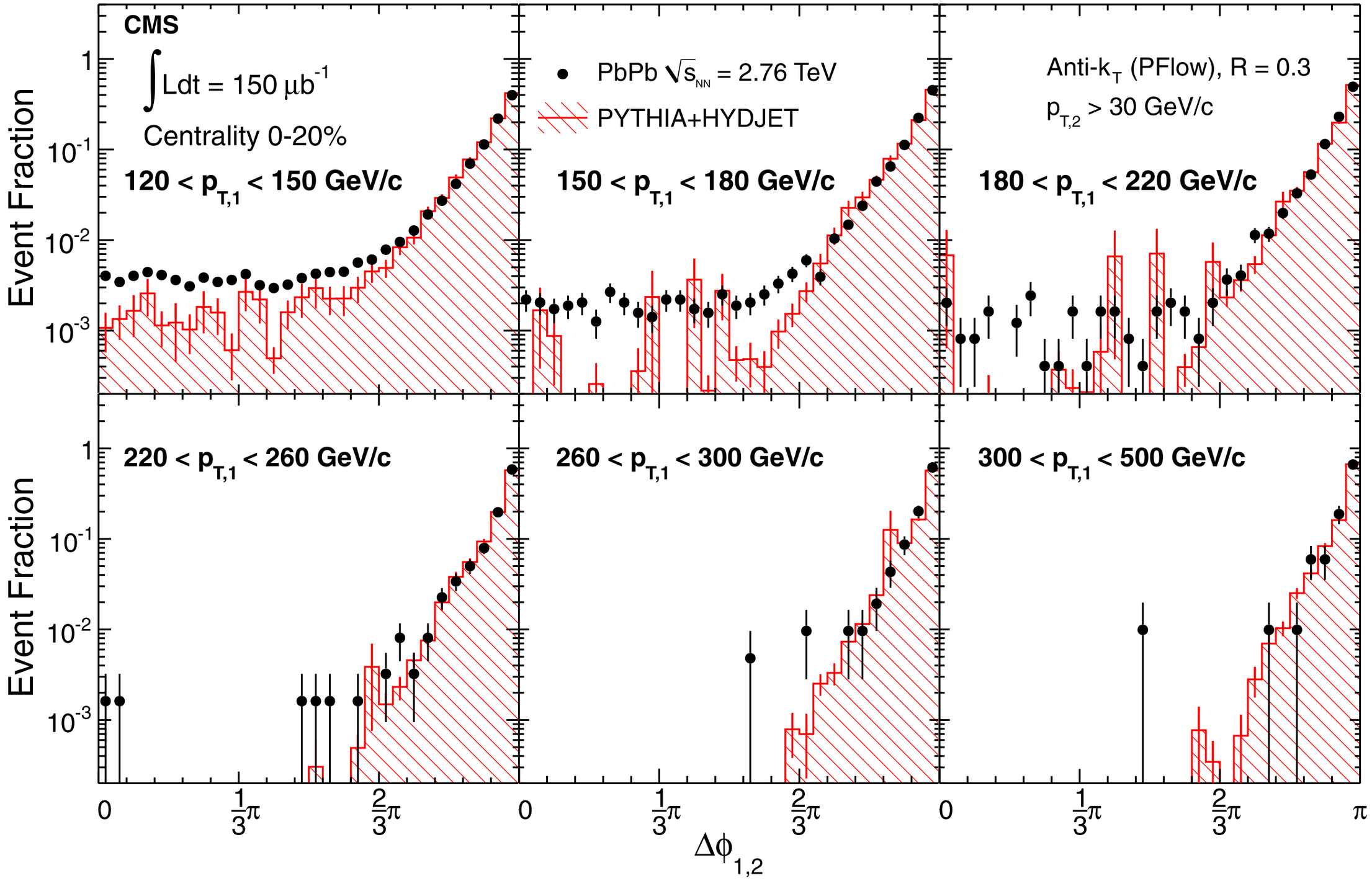

Fig. 1. Distribution of the angle $\Delta\varphi_{1,2}$ between the leading and subleading jets in bins of leading jet transverse momentum from $120 < p_{T,1} < 150$ GeV/c to $p_{T,1} > 300$ GeV/c for subleading jets of $p_{T,2} > 30$ GeV/c. Results for 0–20% central PbPb events are shown as points while the histogram shows the results for pythia dijets embedded into hydjet PbPb simulated events. The error bars represent the statistical uncertainties.

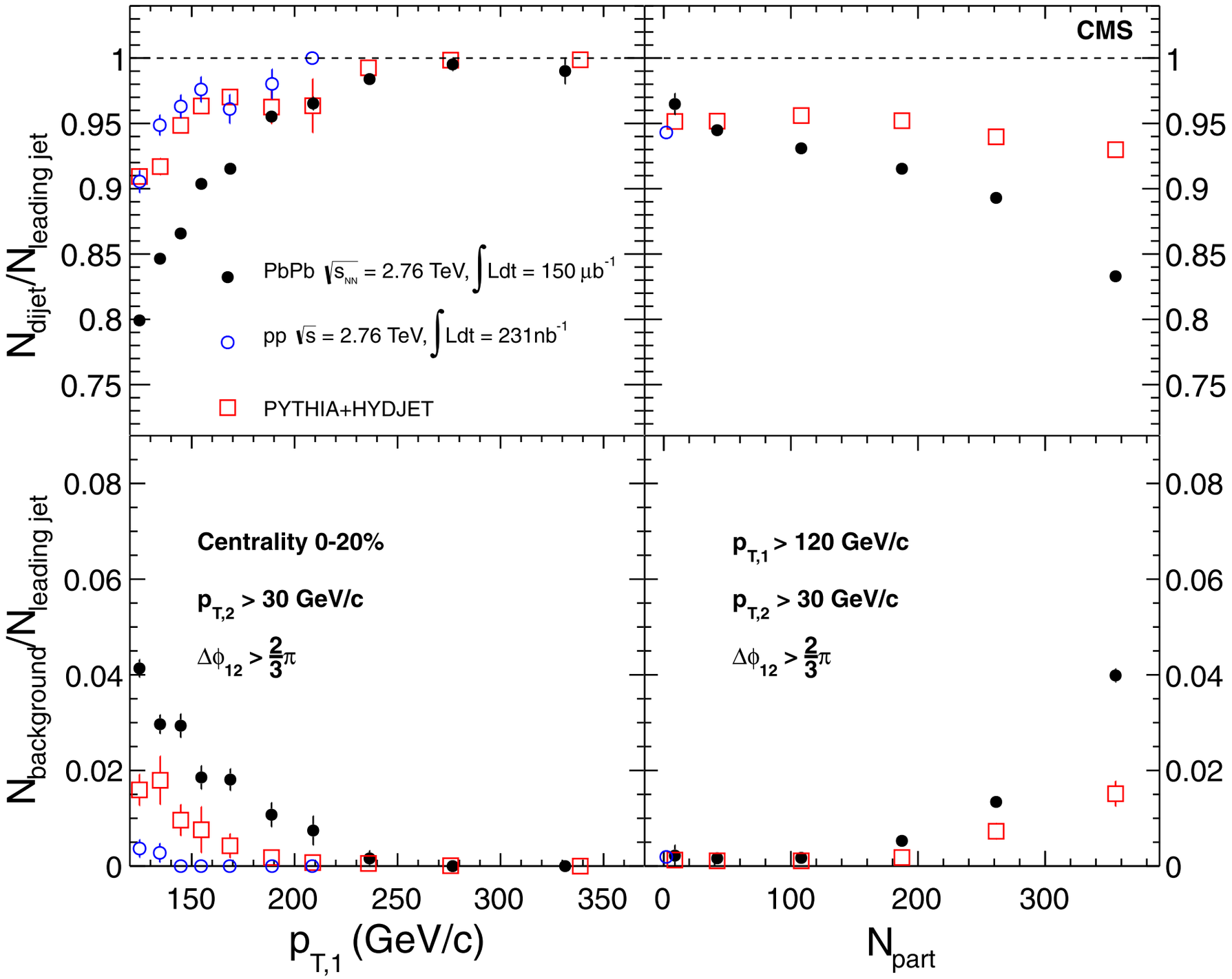

Fig. 2. Fraction of events with a genuine subleading jet with $\Delta\varphi_{1,2} > 2\pi/3$, as a function of leading jet $p_{T,1}$ (left) and Npart (right). The background due to underlying event fluctuations is estimated from $\Delta\varphi_{1,2} < \pi/3$ events and subtracted from the number of dijets. The fraction of the estimated background is shown in the bottom panels. The error bars represent the statistical uncertainties.

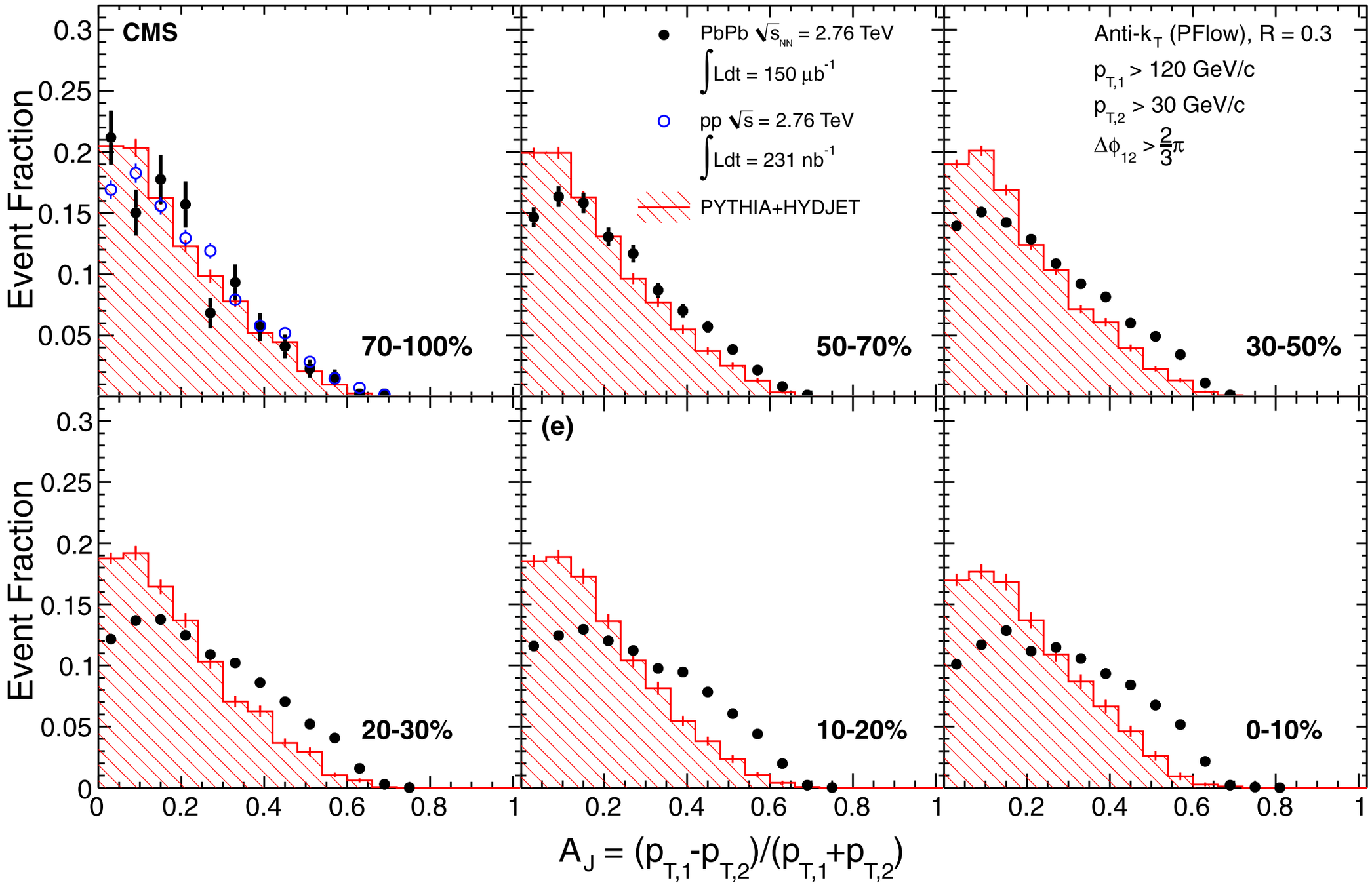

Fig. 3. Dijet asymmetry ratio, A_J , for leading jets of $p_{T,1} > 120$ GeV/c and subleading jets of $p_{T,2} > 30$ GeV/c with a selection of $\Delta\varphi_{1,2} > 2\pi/3$ between the two jets. Results are shown for six bins of collision centrality, corresponding to selections of 70–100% to 0–10% of the total inelastic cross section. Results from data are shown as points, while the histogram shows the results for pythia dijets embedded into hydjet PbPb simulated events. Data from pp collisions at 2.76 TeV are shown as open points in comparison to PbPb results of 70–100% centrality. The error bars represent the statistical uncertainties.

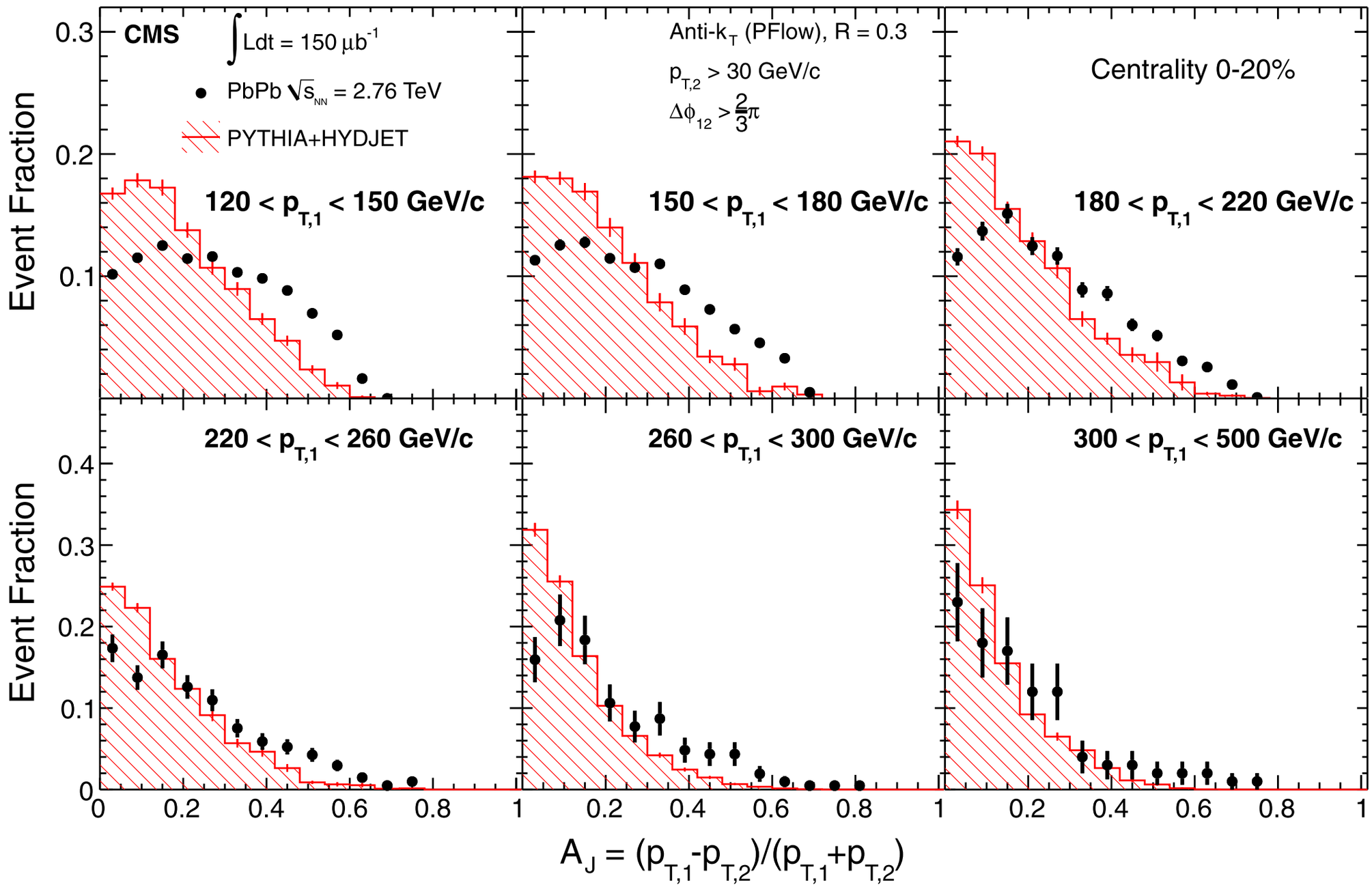

Fig. 4. Dijet asymmetry ratio, A_J , in bins of leading jet transverse momentum from 120 < $p_{T,1}$ < 150 GeV/c to $p_{T,1}$ > 300 GeV/c for subleading jets of $p_{T,2}$ > 30 GeV/c and $\Delta\varphi_{1,2}$ >2π/3 between leading and subleading jets. Results for 0–20% central PbPb events are shown as points, while the histogram shows the results for pythia dijets embedded into hydjet PbPb simulated events. The error bars represent the statistical uncertainties.

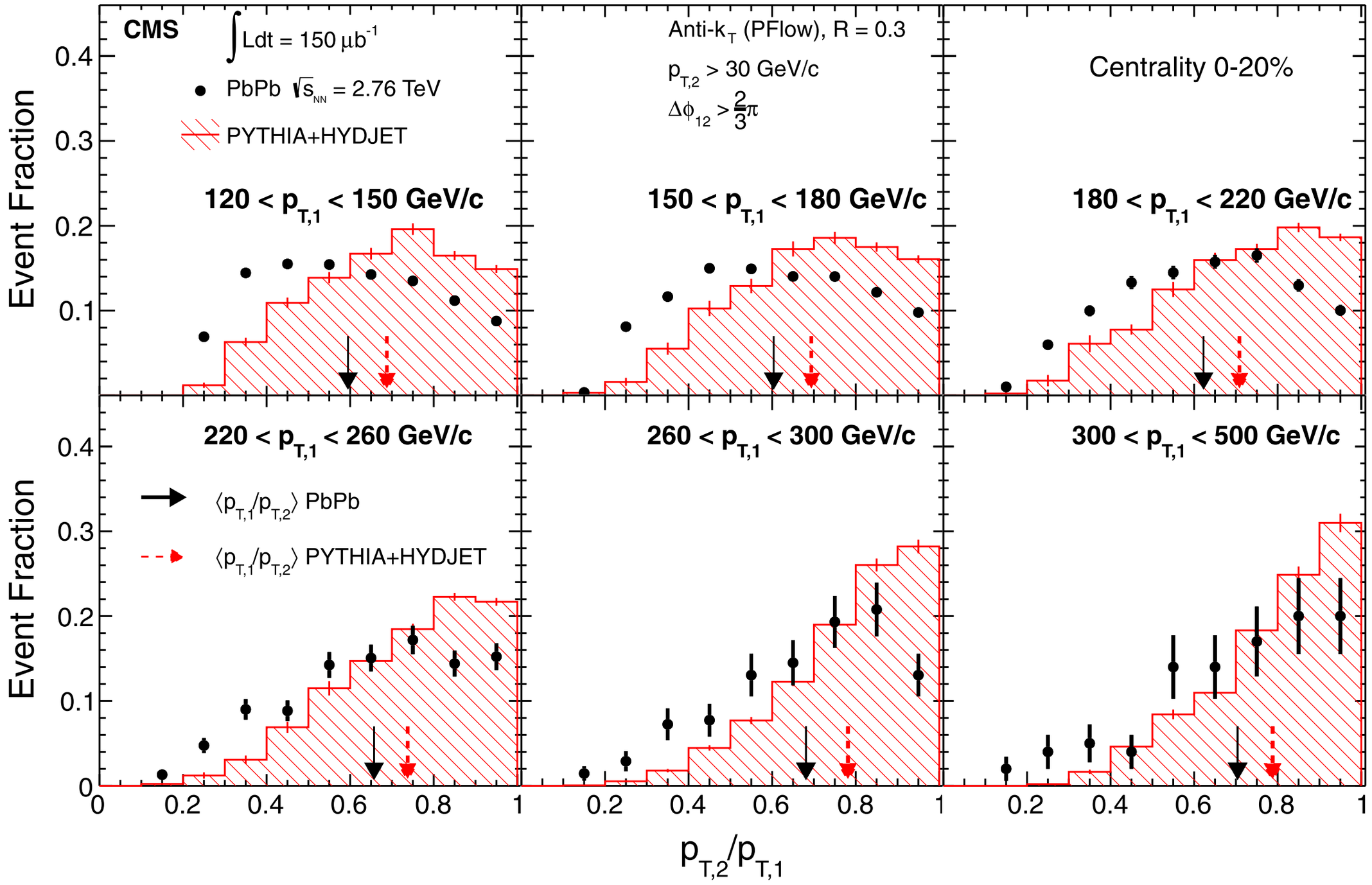

Fig. 5. Subleading jet transverse momentum fraction ($p_{T,2}/p_{T,1}$), in bins of leading jet transverse momentum from 120 < $p_{T,1}$ < 150 GeV/c to $p_{T,1}$ > 300 GeV/c for subleading jets of $p_{T,2}$ >30 GeV/c and $\Delta\varphi_{1,2}$ >2π/3 between leading and subleading jets. Results for 0–20% central PbPb events are shown as points, while the histogram shows the results for pythia dijets embedded into hydjet PbPb simulated events. The arrows show the mean values of the distributions and the error bars represent the statistical uncertainties.

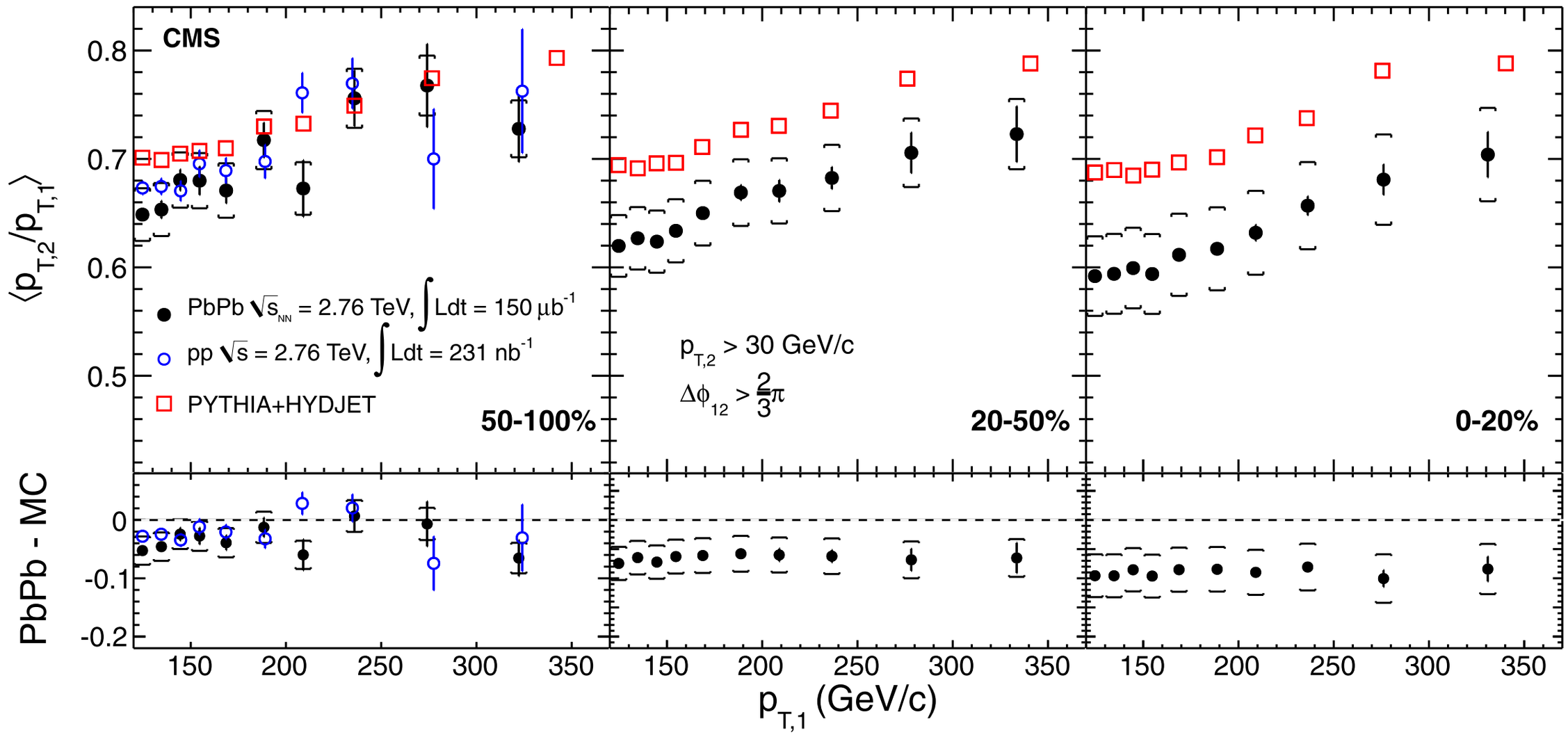

Fig. 6. Average dijet momentum ratio $p_{T,2}/p_{T,1}$ as a function of leading jet p_T for three bins of collision centrality, from peripheral to central collisions, corresponding to selections of 50–100%, 30–50% and 0–20% of the total inelastic cross section. Results for PbPb data are shown as points with vertical bars and brackets indicating the statistical and systematic uncertainties, respectively. Results for pythia+hydjet are shown as squares. In the 50–100% centrality bin, results are also compared with pp data, which is shown as the open circles. The difference between the PbPb measurement and the pythia+hydjet expectations is shown in the bottom panels.